

AERODYNAMIC DISTURBANCE ON VEHICLE'S DYNAMIC PARAMETERS

MU'AZU J. MUSA*, SHAHDAN SUDIN, ZAHARUDDIN MOHAMED

Department of Control and Mechatronics Engineering, Faculty of Electrical Engineering,
Universiti Teknologi Malaysia, Johor Bahru, Malaysia

*Corresponding Author: mjmusa@abu.edu.ng

Abstract

This research paper analysed the influence of aerodynamic disturbance on vehicle's dynamic parameters. The vehicle dynamics were formulated from the Newton's Second Law for modelling the vehicle. The vehicle was built using rigid body frames, mass and multi-body signal blocks of MapleSim2015 platform. Several vehicle masses were used to produce different vehicle dynamics with respect to the same aerodynamic drag and input force. Our analyses have shown that the mass of each vehicle is inversely proportional to the aerodynamic drag applied to it. At a given set-point of 25 ms^{-1} , the vehicle tracked the given speed exactly in the absence of the drag. However, for the lag in displacement, speed and acceleration were found as 25 m , 17 ms^{-1} and 0.3 ms^{-2} , respectively in the presence of drag with an average jerk of 45 ms^{-3} . This has provided an interesting insight on the effects of drag on the moving vehicle. The proposed vehicle was subjected to the same control strategy to form a two-vehicle, look-ahead convoy as in conventional type. Improvements in the inter-vehicular spacing of 1.7 m , proper speed track, low acceleration (1.05 ms^{-2}) and a suitable jerk of 0.04 ms^{-3} were achieved over the entire period (160 s) as compared to conventional vehicle. The proposed vehicle model scores higher accuracy than conventional vehicle on two-vehicle, look-ahead model and it has shown that the proposed model is more comfortable than the conventional one.

Keywords: Acceleration, Aerodynamic, Jerk, Position, Vehicle speed.

1. Introduction

The demand for highway travel keeps on growing as the population rises, especially in urban areas. Construction of new highways to accommodate this growth in traffic density has been dropping behind. The capacity of goods transportation alone has

Nomenclatures	
A	Area of vehicle frontal projection, m^2
a_i	Acceleration of reference i -th vehicle, ms^{-2}
C_D	Air drag coefficient
$F_i(t)$	Applied force, N
$F_d(t)$	Air drag force, N
$F_m(t)$	Moving force, N
g	Gravity, ms^{-2}
H	Spring relationship between i -th and $(i - 2)$ -th vehicle
H_a	Damper relationship between i -th and $(i - 2)$ -th vehicle
$h\dot{x}_i$	Speed dependent spacing policy
K_{pi}	Spring constant
K_{vi}	Damper constant
L	Vehicle length which includes desire inter-vehicular spacing, m
m	Mass of vehicle, kg or Number of the particular vehicle concern
n	Number of vehicles ahead
u_i	Control signal of the baseline vehicle, ms^{-2}
U_i	Control signal of the convoy vehicle, ms^{-2}
W	Weight of vehicle, N
x	Displacement, m
\dot{x}_i	Speed of the i -th vehicle, ms^{-1}
\dot{x}_{i-1}	Speed of the $(i - 1)$ -th vehicle, ms^{-1}
\dot{x}_{i-2}	Speed of the $(i - 2)$ -th vehicle, ms^{-1}
x_i	Position of vehicle i , m
x_{i-1}	Spacing between the predecessor and the control vehicle, m
x_{i-2}	Spacing between the leader and the control vehicle, m
Z	Spring relationship between i -th and $(i - 1)$ -th vehicle
Z_a	Damper relationship between i -th and $(i - 1)$ -th vehicle
Greek Symbols	
v	Terminal velocity, ms^{-1}
ρ	Density of air, kg/m
Abbreviations	
CAD	Computer-aided design
CHT	Constant headway time
VCPS	Vehicular cyber-physical system

been projected to almost double by 2020. The traffic issue is often expected to be a problem of metropolis, but it is also common in rural areas [1]. In the area of vehicle convoy, feasible control is important to ensure smooth traffic flow on the highway. However, the influence of aerodynamic on moving vehicles remains a challenging problem, especially for the convoy.

Aerodynamic drag is inherent in moving vehicles and it needs to be drastically reduced to a bearable level. To achieve this, it is imperative to ensure effective measures be put in place to counter the undesired effects of aerodynamics. This study has focussed on determining the effects of drag on the moving vehicle. This is to show the necessity of including an efficient disturbance rejection technique

to cancel out the influence of drag on the vehicle for an efficient and slinky-effect free vehicle movement.

The air drag on a vehicle has direct impact on its aerodynamics, and may result in amplification of the vehicle's oscillation (i.e. the string instability). The influence of the air drag requires in-depth investigation for proper convoy analyses. In this study, a vehicle with different masses (500 kg, 1000 kg and 1500 kg) were used to represent heterogeneous vehicles. It gives us a real scenario where vehicles of different dynamics are involved and allows us to compare the effects of such drag. Variation in vehicle mass may occur due to loading/unloading of goods/passengers and fuel consumption condition. The changes in the vehicle mass may significantly contribute to changes in an individual vehicle's dynamics and the entire string of the convoy during sudden break and acceleration of leading vehicle [2].

An overview on vehicular convoy conducted by [2] presented a survey on a platoon-based vehicular cyber-physical system (VCPS). Their work reviewed relevant works of platoon-based VCPS and made suggestions on important issues that could open new research direction in the field, such as investigating the effects of external forces. The survey on vehicle platoon was conducted by [3] considering vehicular platoon management methods from the angle of networked control. The research analysed the problem of string instability due to rapid propagation of errors in the strings of convoy as a result of neglecting the effects of external forces and concluded that the existing vehicle convoy suffered greatly from air drag force.

Cloudin and Komathy [4] developed a mobility model for vehicular networks, which was aimed at enhancing string stability in line with network performance. The co-operative controller designed in the work did not consider the effects of drag that could bring about sudden change in the vehicle's dynamics, leading to poor performance of the controller in terms of string stability. A two-vehicle, look-ahead control strategy was proposed and investigated by [5]. The model's formulation is the same as that of [6] and also did not consider the effects of external forces on the baseline vehicle. Ali et al. [7] proposed a model for flatbed platoon for safety improvement in dense convoys on highways, specifically to enhance inter-vehicle spacing. The model also did not consider the effects of drag leading to the possibility of string instability. Other such insufficient models include those in [8-10]. Our research work does focus on analysing the effects of disturbance on vehicle's position, speed, acceleration and jerk. Hence, the main contribution of this work is to investigate the effects of aerodynamic disturbance (i.e., the drag) on vehicle dynamics. This was achieved by developing a mathematical model to enable visualisation of the effects of the drag and to suggest feasible ways of mitigating it.

The remainder of this paper describes modelling and formulation in Section 2, while Section 3 analyses the influence of aerodynamic disturbance on the vehicle and effects of the vehicle in a convoy will be shown. Lastly, Section 4 concludes on the analysed results.

2. Materials and Methods

The proposed methodology has utilized MAPLE2015 and MapleSim2015 platforms for modelling in this study.

Consider a vehicle with mass m and external force $F_i(t)$ acting on it to cause a displacement x in the direction of motion. There exists an air drag force $F_d(t)$, which opposes the vehicle's motion, resulting in final vehicle moving force $F_m(t)$, as shown in Fig. 1.

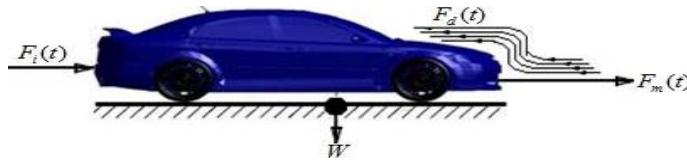


Fig. 1. Vehicle input, moving force and disturbance.

The model takes into account the air drag. In Fig. 1, the following relationship holds:

$$F_i(t) = F_d(t) + F_m(t) \quad (1)$$

where $F_i(t)$ is the applied force; $F_d(t)$ is the air drag and $F_m(t)$ the vehicle moving force.

The applied input force $F_i(t)$ is the combination of step input so chosen to feed into the vehicle model to enable motion, while $F_d(t)$ is the air drag acting against the vehicle and it is expressed as [11].

$$F_d(t) = \frac{1}{2} \rho \left(\frac{d}{dt} S(t) \right)^2 C_D \times A \quad (2)$$

Here, C_D is the air drag coefficient; A is the area of vehicle frontal projection and ρ is the density of air.

Rearranging Eq. (1) and hence $F_m(t)$ can be expressed as

$$F_m(t) = F_i(t) - F_d(t) \quad (3)$$

The vehicle moving force is the product of the vehicle's mass and its acceleration, neglecting the air drag yields [5]

$$F_i(t) = m a_i \quad (4)$$

where a_i is the acceleration of reference i – th vehicle.

$$a_i = \frac{1}{m} [F_i(t)] \quad (5)$$

$$a_i = \frac{1}{m} [m u_i] \quad (6)$$

Here, u_i is the control signal.

$$W = mg \quad (7)$$

In Eq. (7), W is the weight of the vehicle in kg.

Equation (6) clearly shows the control signal of the vehicle, which is modelled as an inertial mass with direct influence on its applied force, as seen in the equation by considering the fact that the following vehicle has no impact on their neighbouring vehicles [12]. The weight of vehicle W is constant at rest; it

depends on individual vehicle dynamics, which varies during loading and unloading and also due to fuel consumption.

The net external force shown in Eq. (1) is the summation of the two forces, F_d and F_m . Since air drag is neglected, we therefore have

$$F_i = F_m \tag{8}$$

Since the air drag (F_d) acting against the vehicle is neglected in Eq. (3), hence Eq. (4) yields the following, while Eq. (10) is the final acceleration:

$$F_m = ma \tag{9}$$

$$a = \frac{F_m}{m} = \frac{F_i}{m} \tag{10}$$

On the other hand, the terminal velocity (v) is given as:

$$v = \frac{F_m}{m} t \tag{11}$$

2.1. Vehicle modeling procedure

The model was built on Maple/MapleSim2015 platform following the derivation of vehicle dynamics. The signal blocks, multibody components, sensors and Computer-aided design (CAD) visualization were used to model the vehicle, while customized component was created for the drag force on Maple. Parameterization, such as mass of vehicle ' m ', air drag coefficient ' C_D ', area of vehicle frontal projection ' A ' and density of air ' ρ ' were incorporated. Subsequent changes in mass were carried out to create different vehicle loading scenarios. Figure 2 below shows the complete vehicle model.

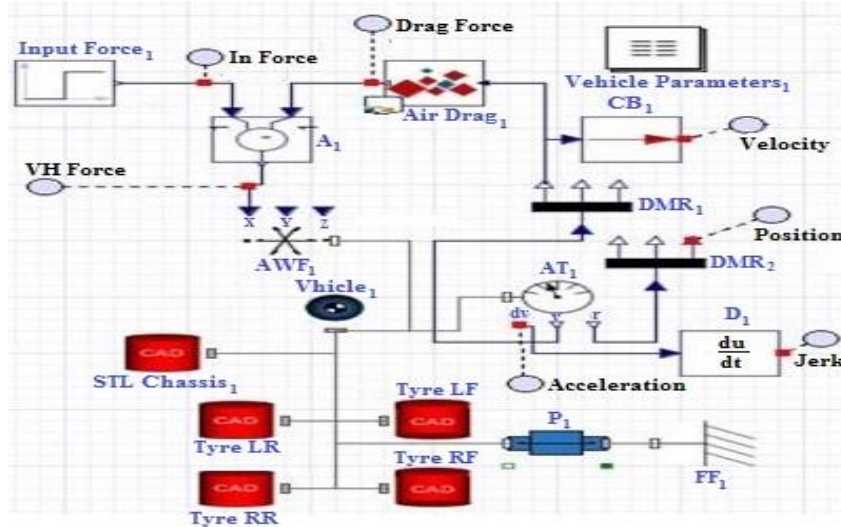


Fig. 2. Complete vehicle model on MapleSim2015 platform.

2.2. Two-vehicle, look-ahead control strategy modeling procedure

To enable comparing the proposed vehicle model with that of [6], we need to form similar control strategy with different vehicle model and drag, which consists of the predecessor and lead vehicle. Eq. (13) shows the communication flow of the two-vehicle look-ahead as seen in Fig. 3.

Here, \dot{x}_i , \dot{x}_{i-1} and \dot{x}_{i-2} are the respective speeds of i -th, $(i-1)$ -th and $(i-2)$ -th vehicle.

$$\left. \begin{aligned} \mathbf{Z} &= \mathbf{K}_{p1}(x_{i-1} - x_i - h\dot{x}_i), \mathbf{Z}_a = \mathbf{K}_{v1}(\dot{x}_{i-1} - \dot{x}_i), \\ \mathbf{H} &= \mathbf{K}_{p2}(x_{i-2} - x_i - 2h\dot{x}_i), \mathbf{H}_a = \mathbf{K}_{v2}(\dot{x}_{i-2} - \dot{x}_i) \end{aligned} \right\} \quad (12)$$

$$\mathcal{U}_i = \mathbf{Z} + \mathbf{H} + \mathbf{Z}_a + \mathbf{H}_a \quad (13)$$

In Eqs. (12) and (13) above, \mathcal{U}_i is the control signal of the convoy, $h\dot{x}_i$ is the speed dependent spacing policy, the Constant headway time (CHT). As the convoy speed increases, the inter-vehicular spacing increases and vice versa. When the vehicles in the convoy are moving at steady speed, it is assumed that the inter-vehicular spacing between the predecessor vehicle (x_{i-1}) to the control vehicle (x_i) is half of the leader vehicle (x_{i-2}) to the control vehicle.

While the following constrains were maintained, Eq. (14) is the constraint, which provides the control vehicle with the information of predecessor vehicle. The control vehicle uses the information to make necessary adjustments on speed for safety inter-vehicular spacing between them.

$$x_i \leq x_{i-1} - h\dot{x}_i \quad (14)$$

Equation (15) is the constraint, which provides control vehicle with the information of the leader vehicle. The control vehicle uses the information to make necessary adjustments on speed for safety inter-vehicular spacing between them.

$$x_i \leq x_{i-2} - 2h\dot{x}_i \quad (15)$$

The control vehicle is fed with the signals from the two vehicles in front. Hence Eq. (13) can be re-written as follows [13]:

$$\mathcal{U}_i = \sum_{m=1}^{n=2} [K_{pm}(\delta_{im} - mh\dot{x}_i) + K_{vm}(\dot{x}_{i-m} - \dot{x}_i)] \quad (16)$$

where,

$$\delta_{im} = \sum_{l=0}^{m-1} \varepsilon_{i-l} = x_{i-m} - x_i - mL \quad (17)$$

where L is the vehicle length which includes desire inter-vehicular spacing and is the same to all the vehicle in our case, m is the number of the particular vehicle concern, n is the number of vehicles ahead.

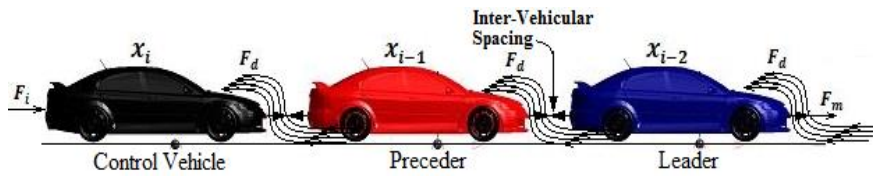


Fig. 3. The proposed vehicle with the two look-ahead control strategies.

3. Results and Analysis

The simulation results of the vehicle under different masses are shown in Figs. 4 through 6. The vehicle air drag depends directly on the square of the vehicle velocity [14]. Therefore, as the vehicle accelerates, its velocity and the drag rise due to the ambient air resistance. There would be a point where the drag equals the vehicle opposing force, hence no net force acting on the vehicle and this results zero acceleration. It can also be seen from Eq. (1) and Figs. 4 to 6 that different masses were used such that an increase or decrease in vehicle mass causes a decrease or increase in drag force, respectively. Since the force has direct impact on the vehicle dynamics, the effects of air drag on any vehicle should not be neglected. The baseline vehicle model of Sudin [6] was tested with the same drag force, $C_D = 0.5$, $\rho = 1.22$ and $A = 1$ to enable proper evaluation of the proposed model.

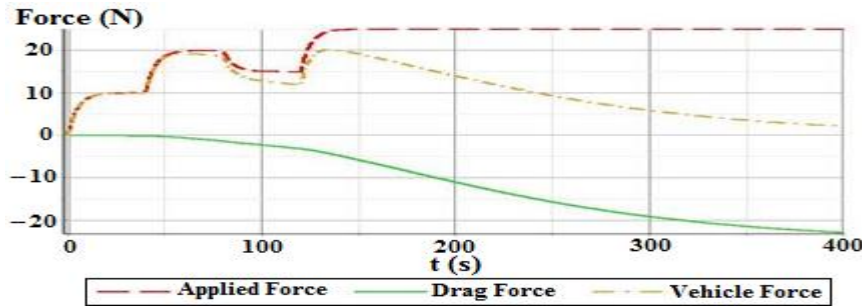


Fig. 4. Applied, drag and vehicle forces of 500 kg vehicle mass.

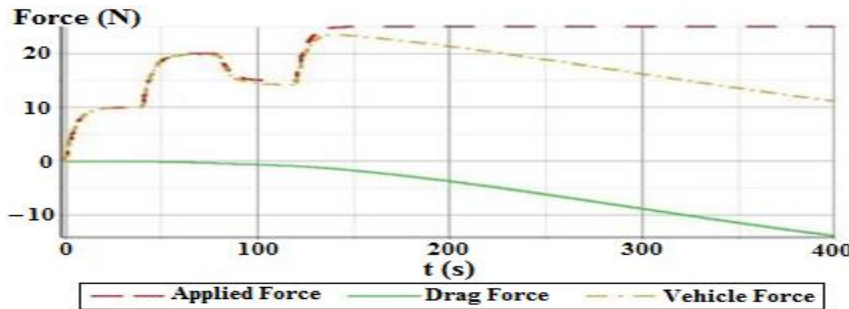


Fig. 5. Applied, drag and vehicle forces of 1000 kg vehicle mass.

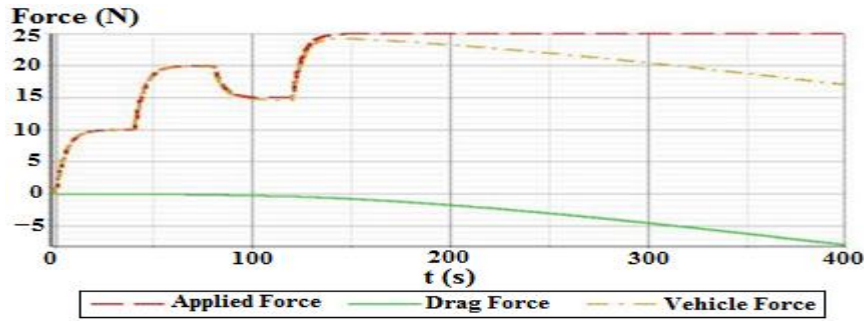


Fig. 6. Applied, drag and vehicle forces of 1500 kg vehicle mass

In Fig. 7, the input-speed has superimposed exactly on the output-speed, it means that the output-speed has instantly attained the input-speed without any time delay. Similar overlap in input and the output speed was achieved in the baseline vehicle model of [6] and this tally with an ideal situation in the absence of air drag.

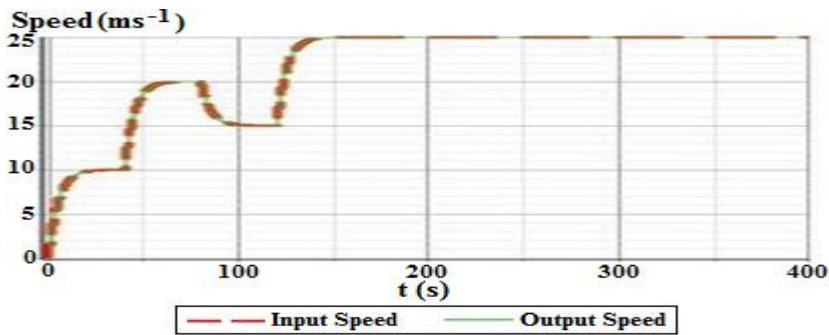


Fig. 7. Input and output speeds of the vehicle without disturbance.

In Fig. 8, the output-speed has same trend with the input-speed, but with a speed delay of 17 ms⁻¹ between the two speeds. This occurs due to the influence of air drag on the vehicle. A speed delay of 17.46 ms⁻¹ was observed from baseline vehicle of [6] in the presence of drag force. This shows that the proposed vehicle model is able to withstand the effects of the applied drag force compared to that of [6] with a speed difference of 0.46 ms⁻¹.



Fig. 8. Input and output speeds of the vehicle with disturbance.

Figure 9 clearly indicates the variation obtained with respect to the vehicle positions on the effects of air drag. Due to the effects of air drag, the vehicle has covered a distance of 1252 m in 200 s, while a distance of 3650 m was covered in the same time of 200 s when no disturbance was assumed. In [6] a distance of 1228.695 m and 3634.718 m were recorded in 200 s with and without air drag forces, respectively. This demonstrates that the influences of air drag on the proposed vehicle and that of Sudin [6] with an undesirable distance lag of 2398 m in 200 s and 2408.023 m, respectively. This means that the proposed vehicle model is better in overcoming the effects of air drag distance by 10.023 m less, as compared with that of [6].

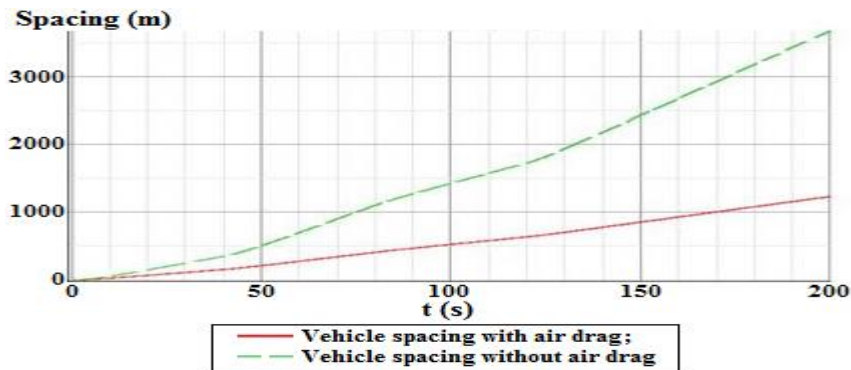


Fig. 9. Vehicle position with and without disturbance.

Figure 10 below shows the effects of air drag on acceleration and deceleration on the vehicle. An acceleration and deceleration lags of 0.3 m/s^2 and 0.8 m/s^2 were obtained respectively in 400 s. This leads to an increase in the vehicle jerk, resulting in some discomfort due to the undesired vibrations. The acceleration and deceleration lags of 0.67 ms^2 and 0.489 ms^2 respectively were recorded [6] in 400 s. This shows that the vehicle in [6] is more uncomfortable than the proposed vehicle model due to the huge difference in both acceleration and deceleration in [6].

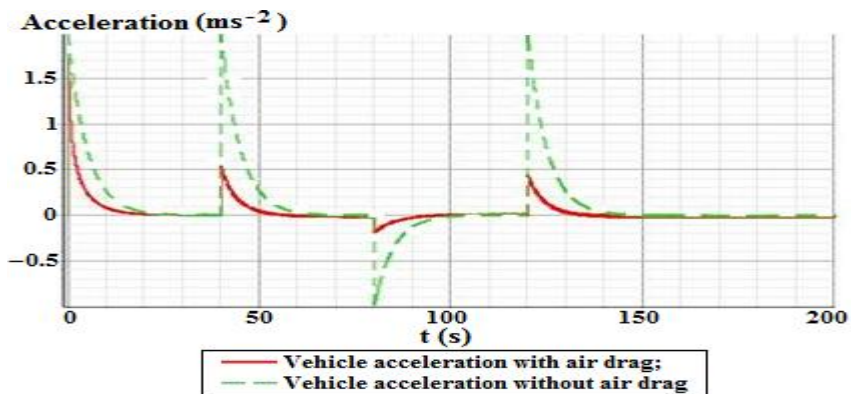


Fig. 10. Vehicle acceleration with and without disturbance.

Figure 11 reveals how the vehicle jerk reacts to the change in air drag. A jerk is defined as the rate of change of acceleration with respect to time. Changes in acceleration at a suitable rate (that is, suitable jerk) are the cause of vibrations, and the vibrations significantly impair the quality of transportation [15]. The same figure shows a maximum jerk of 45 m/s^3 due to air drag, which is larger than the rated jerk value, i.e., $\frac{3}{4}$ acceleration that produces it [6]. Hence, there is a good reason to minimize disturbance in transportation vehicles. Meanwhile, a maximum jerk of 1.709 m/s^3 was recorded in the vehicle of [6], which is larger than that obtained using the proposed model and also larger than the rated jerk with respect to the model's acceleration. In the absence of air drag, vertical lines were seen, this was caused by the differential overshoots inherent in the vehicle's acceleration. Such overshoots can be eliminated by incorporating filters in the design.

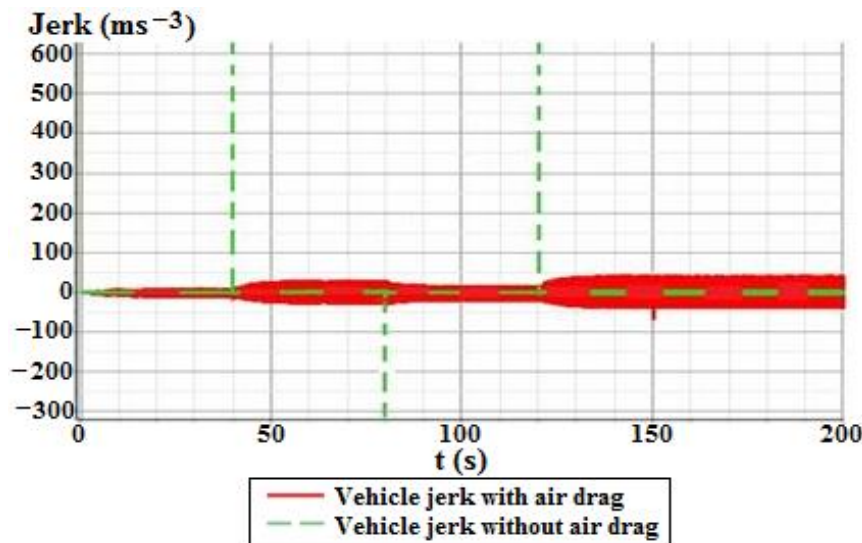


Fig. 11. Vehicle Jerk with and without disturbance.

Figure 12 presents the proposed vehicle model used to compare with [6] to justify the acquired improvements of the proposed vehicle model. The proposed vehicle was subjected to similar control strategy to experience and receive similar information as [6]. It permits smooth and free running of the vehicle over a period of 160 s' test with maximum spacing of 145 m. This speed dependent policy gives a wider range of inter-vehicular spacing at maximum 35 m apart; it also permits the control vehicle to react to sudden changes on speed of other vehicles. As seen in this figure, the maximum spacing of the proposed model prevents collision among the stream of vehicles due to wide spacing apart when it accelerated and vice versa. On the contrary, [6] has the following shortcomings of chattering for the first 70 s and with maximum spacing of only 33.3 m apart, which indicated the possibility of collision among the vehicles at high speed. The two models ran for 160 s but [6] was only visible for the first 115 s and truncated for the last 45 s due to the ill condition of the vehicle, while the proposed model ran efficiently for the whole period.

Figure 13 shows how the control of the proposed vehicle model closely tracks the path of leader and predecessor vehicles without collision. This shows the ability of the control vehicle depends mainly on the acceleration, deceleration and constant speed of the neighbouring vehicles within the convoy as compared to [6]. The conventional vehicles show lapses in speed within the vehicles. The speed has also been affected by the chattering effects even at low speed of 25 ms^{-1} within the first 70 s. The resulted chattering effects to an overlap in speed among the vehicles. The convoy speeds of [6] truncated for the last 45 s. This gives a blank picture for the convoy speed in the remaining 45 s, hence no account of the convoy for this period is known.

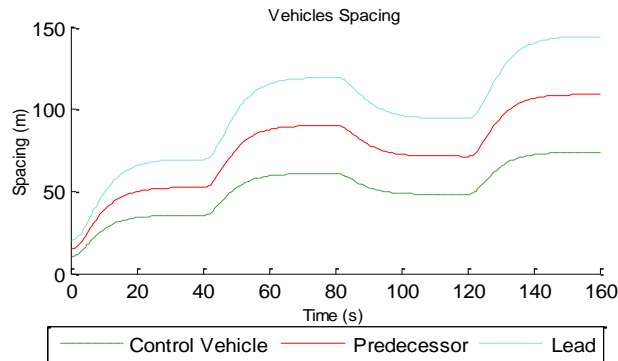


Fig. 12. Position of the proposed vehicle used as a two look-ahead convoy.

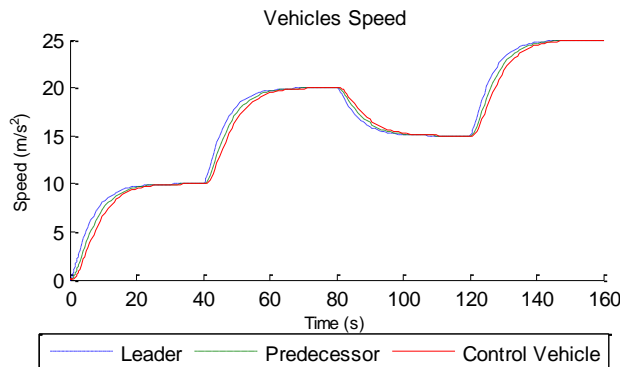


Fig. 13. Speed of the proposed vehicle used as a two look-ahead convoy.

Figure 14 shows the rate of change of the control vehicle's velocity within the convoy maintained at maximum acceleration of 1.05 ms^{-2} , which is below the maximum acceptable acceleration of 2 ms^{-2} [16] and minimum deceleration of 0.4 ms^{-2} . The control vehicle's acceleration was maintained within safe operation range as indicated by the constraint Eqs. (14) and (15). Its acceleration did not cross or overlap any independent vehicles within the convoy. This shows proper vehicle control as compared to [6]. It is evident that inconsistent acceleration was observed in the control vehicle in [6]. This variation in the rate

of change of velocity of the control vehicle was seen at the first 70 s when controlled with maximum acceleration of 1.1 ms^{-2} and minimum deceleration of 0.4 ms^{-2} . This was also an outstanding achievement but the shortcoming of this acceleration has caused chattering phenomena, which ran for only 70 s from the start and the whole journey discontinued at 115 s of the running time of 160 s. The maximum acceleration of the control vehicle in [6] was high (1.1 ms^{-2}) compared to that of the proposed vehicle (1.05 ms^{-2}). This slight difference in the control vehicle's acceleration in both cases has significant effect on final control of the vehicle's jerk, in which the overall passenger comfort depends on.

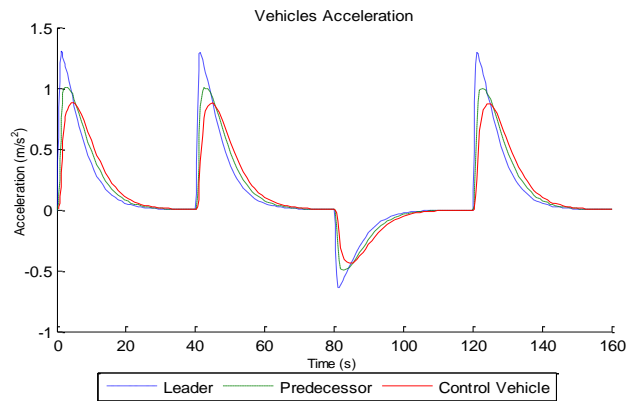


Fig. 14. Acceleration of the proposed vehicle used as a two look-ahead convoy.

Among other factors, the passenger's comfort also depends on the vehicle's jerk. The smaller the jerk, the more comfortable the vehicle will be. The jerk of the proposed control vehicle in Fig. 15 is 0.43 m/s^3 , which is pretty low and far from the maximum rated jerk of 5 m/s^3 [17, 18]. This value signifies that the control vehicle would be comfortable for passengers [6]. On the contrary, [6] shows rapid response of undesirable jerk of 0.47 m/s^3 . The undesired oscillation produced in the simulation was due to the fact that small oscillation has occurred as the vehicle was trying to settle down at its final speed in [6]. The jerk is higher than the proposed vehicle by as much as 0.04 m/s^3 . This difference on the jerk, in addition to the oscillation, would lead to passengers' discomfort significantly.

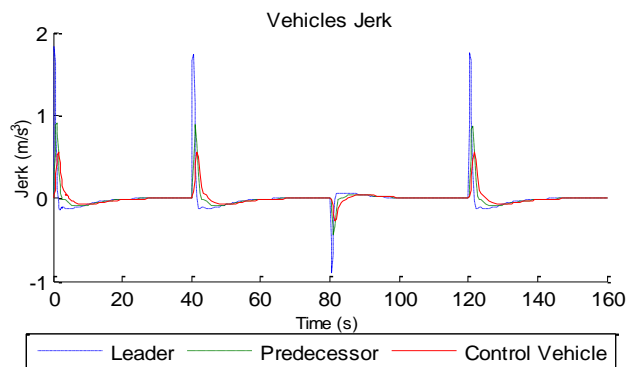


Fig. 15. Jerk of the proposed vehicle used as a two look-ahead convoy.

4. Conclusions

In this study, a single vehicle model has been developed and examined to provide detailed knowledge on the influence of aerodynamics on vehicle motion with respect to its dynamic parameters. The study provides suitable information and emphasized on the effects of drag force against moving vehicle for precise results. A clear distinction was drawn from the delay observed in all the vehicles' dynamic parameters, as compared to that of [6] with the presence of air drag disturbance, that the proposed vehicle model is more practical and accurate than that of [6]. These observed delays on various parameters have indicated how vehicle suffer from a lot of setbacks to reach its destination. Hence, there is need to greatly minimize the effects of air drag against moving vehicle to travel a distance of 3650 m in 200 s, at a speed of 25 ms⁻¹ in 400 s, at the acceleration of 1.98 m/s² in 200 s, and the jerk of three-quarter of the overall vehicle's acceleration in 200 s. When the optimized dynamics values were achieved, the vehicle will benefit from an increase in speed with reduced jerk. Further steps were taken to examine the vehicle's dynamic parameters in a convoy of a two-vehicle, look-ahead formation and it has been found that the proposed vehicle was free from chattering and continued throughout the journey. It maintained better inter-vehicular spacing (35 m) than that of [6], which suffered much more chattering, with only 33.3 m inter-vehicle spacing and truncated for the last 45 s. It was observed that the proposed vehicle tracked the path of its neighbouring vehicles; on the contrary a lot of lapses in speed were experienced in [6]. Higher maximum acceleration (1.1 m/s²) was recorded as compared to the proposed vehicle with only 1.05 m/s². The change in maximum acceleration has led to undesired vibration in the control of the vehicle's jerk. The jerk of the control vehicle in [6] was found to be 0.04 ms⁻³, greater than that of the proposed control vehicle. This has justified that the proposed vehicle is good enough to improve the overall vehicle convoy's performance and would result to continuous and free chattering vehicle convoy system.

References

1. Rich, T. (2012). Urban congestion trends operations: The key to reliable travel. *U.S. Department of Transportation, Federal Highway Administration*, U.S, 1-5.
2. Jia, D.; Lu, K.; Wang, J.; Zhang, X.; and Shen, X. (2016). A survey on platoon-based vehicular cyber-physical systems. *IEEE 2016 Communications Surveys & Tutorials*, 18, 263-284.
3. Li, S.E.; Zheng, Y.; Li, K.; and Wang, J. (2015). An overview of vehicular platoon control under the four-component framework. In: *IEEE 4th Intelligent Vehicles Symposium*. Seoul, South Korea, 286-291.
4. Cloudin, S.; Komathy, K. (2013). Performance analysis of fuzzy co-operative adaptive Cruise controller in vehicular Ad Hoc networks. In: *IET Sustainable Energy and Intelligent Systems Conference*. Chennai, Tamil Nadu, India, 329-325.
5. Hassan, A.U.; and Sudin, S. (2015). Road vehicle following control strategy using model reference adaptive control method stability approach. *Jurnal Teknologi (Sciences & Engineering)*, 72, 111-117.

6. Sudin, S.; and Cook, P.A. (2004). Two-vehicle look-ahead convoy control systems. In: *IEEE 56th Vehicular Technology Conference*. Milan, Italy, 2935-2939.
7. Ali, A.; Garcia, G.; and Martinet, P. (2015). The flatbed platoon-towing model for safe and dense platooning on highways. *IEEE Intelligent transportation systems magazine*, 7(1), 58-68.
8. Asplund, M. (2015). Model-based membership verification in vehicular platoons. In: *IEEE International Conference on Dependable Systems and Networks*. Rio de Janeiro, Brazil, 125-132.
9. Jing, J.; Kurt, A.; Ozatay, E.; Michelini, J.; Filev, D.; Ozguner, U. (2015). Vehicle speed prediction in a convoy using V2V communication. In: *IEEE Intelligent Transportation Systems*. Las Palmas, Spain, 2861-2868.
10. Marjovi, A.; Vasic, M.; Lemaitre, J.; and Martinoli, A. (2015). Distributed graph-based convoy control for networked intelligent vehicles. In: *IEEE 4th Intelligent Vehicles Symposium*. Seoul, South Korea, 138-143.
11. Sarafian, H. (2015). Impact of the drag force and the Magnus effect on the trajectory of a baseball. *World Journal of Mechanics*. 49-58.
12. Khan, M.; Turgut, D.; and Bölöni, L. (2008). A study of collaborative influence mechanisms for highway convoy driving. In: *Proceedings of International Workshop on Agents in Traffic and Transportation, in conjunction with the Seventh Joint Conference on Autonomous and Multi-Agent Systems*. Estoril, Portugal, 46-53.
13. Cook, P.A.; Sudin, S. (2002) Dynamics of Convoy Control Systems. In: *IEEE 10th Mediterranean Conference on Control and Automation*. Lisboa, Portugal, 1-8.
14. Falkovich, G. (2011). *Fluid Mechanics: Short Course for Physicists*. Cambridge University Press, Cambridge, UK.
15. Sprott, J.S. (1997). Some simple chaotic jerk functions. *American Journal of Physics*, 65, 537-543.
16. Li, P.; Alvarez, L.; and Horowitz, R. (1997). AHS Safe Control Laws for Platoon Leaders. In: *IEEE Transactions on Control System Technology*, 5(6), 614-628.
17. Godbole, D.N.; Lygeros, J. (1994) Longitudinal Control of the Lead Car of a Platoon. In: *IEEE Transactions on Vehicular Technology*. Baltimore, MD, USA. 398-402.
18. Musa, M. J. Sudin, S. Mohamed, Z. and Nawawi, S. W. (2017). Novel Information Flow Topology for Vehicle Convoy Control. In Mohamed Ali, M. S. Wahid, H. Mohd Subha, N. A. Sahlan, S. Md. Yunus, M. A. Wahap, A. R. (Eds.), *Modelling, Design and Simulation of Systems*. AsiaSim2017. *Communications in Computer and Information Science*, Springer Nature, Gateway East, Singapore, Aug. 26, 2017. 751: (pp. 323-335). Gateway East, Singapore: Springer Nature.